DARCY-FORCHHEIMER CHARACTERISTICS OF VISCOELASTIC STRATIFIED NANOLIQUID BY CONVECTIVELY HEATED PERMEABLE SURFACE

by

Muhammad Adil SADIQ [a], ***Muhammad WAQAS*** [b*], ***and Tasawar HAYAT*** [c,d]

[a] Department of Mathematics, DCC-KFUPM, Dhahran, Saudi Arabia
[b] NUTECH School of Applied Sciences and Humanities, National University of Technology, Islamabad, Pakistan
[c] Department of Mathematics, Quaid-I-Azam University, Islamabad, Pakistan
[d] Department of Mathematics, Non-Linear Analysis and Applied Mathematics (NAAM) Research Group, Faculty of Science King Abdulaziz University, Jeddah, Saudi Arabia

Original scientific paper
https://doi.org/10.2298/TSCI190708387A

A non-linear mathematical analysis for non-Darcian magneto-viscoelastic nanoliquid is elaborated in this research. Flow is caused by stratified surface having permeable nature. The Robin's type boundary conditions are imposed at moving surface. Brownian diffusion, heat source and thermophoretic aspects are accounted. Complex systems are simplified through the well-known boundary-layer concept which is subsequently transfigured to ordinary ones via transformation technique. Furthermore the meaningful physical variables arising in non-dimensional problems are elucidated via graphs.

Key words: *viscoelastic stratified nanoliquid, permeable surface, thermophoresis, Brownian movement, Heat generation,*

Introduction

It is well-known that orthodox heat transferring materials for illustration water, ethylene-glycol (EG) and mineral oil have inadequate heat transport characteristics in comparison solids. An innovative approach regarding liquids heat transport is to adjourn smaller solid elements in liquids. This innovative class of liquid identified as nanoliquid was firstly elaborated by Choi and Eastman [1]. Nanoliquid elaborates a solid-liquid concoction comprising fundamental lower volume fraction having higher conductivity solid nanoparticles. Such liquids have ample uses for instance melt-spinning, production of glass-fiber, airplanes and micro-reactors, *etc.* Researchers considered nanoliquid mechanisms like thermal diffusion, thermophoretic, particle-particle coupling, Brownian movement, micro-convection, and conduction subjected to aggregates. Some experimental researches declare nanoparticles Brownian movement is leading aspect that significantly affect liquids thermal competence. Few recent analyses featuring nanoliquid dynamics under distinct characteristics are mentioned in [2-10].

* Corresponding author, e-mails: mwaqas@math.qau.edu.pk; muhammadwaqas@nutech.edu.pk

Another appealing approach for heat transference improvement in industrial structures is the consideration of porous medium for illustration, the utilization of porous materials based on metal like copper froths in heat exchangers and channel. Indeed porous medium encompasses of miniscule stomas in which liquid-flows. Solar receivers, energy storage units and extraction/percolation of oil through wells are prospective utilizations of such phenomenon. Recently the procedure of implementing both nanoliquid and porous medium has greeted massive consideration and has directed to ample researches in this domain. Nanoparticles disseminated in nanoliquid augment the effective conductivity while porous media upsurges the surface area in relation solid surface and liquid. Consequently it appears that utilizing both nanoliquid and porous media can raise the effectiveness of standard thermal system meaningfully [11].

Aforementioned analyses witness that nanoliquid and porous medium are considered for viscous liquid situation. Here we aimed to account porous medium aspect employing generalized Darcy relation for hydromagnetic nanoliquid-flow considering viscoelastic (second-grade) liquid. Such consideration is in fact the modification of Darcy expression through boundary features and inertia. Such characteristics cannot be overlooked at higher flow rate. Numerous investigators implemented this relation for flow analysis, for detail see [12-20]. Present research further includes double stratification, suction/injection, heat generation and convective conditions. The HAM [21-25] is opted to achieve non-linear convergent problems. Furthermore the meaningful variables arising in formulated problem are elucidated through graphs.

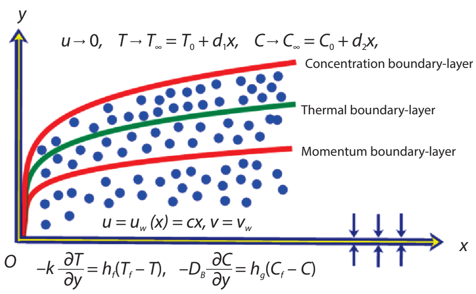

Figure 1. Physical configuration

Formulation

An incompressible viscoelastic (second-grade) liquid-flow by permeable stratified surface is formulated. Hydromagnetic characteristics are accounted for flow analysis. The Robin's type boundary conditions in addition double stratification are imposed at moving surface, fig. 1. Brownian diffusion, heat source and thermophoretic aspects are retained. By employing overhead suppositions, we have:

$$\frac{\partial u}{\partial x}+\frac{\partial v}{\partial y}=0 \tag{1}$$

$$u\frac{\partial u}{\partial x}+v\frac{\partial u}{\partial y}+\frac{\alpha_1}{\rho_f}\left(u\frac{\partial^3 u}{\partial x\partial y^2}-\frac{\partial u}{\partial y}\frac{\partial^2 u}{\partial x\partial y}+v\frac{\partial^3 u}{\partial y^3}+\frac{\partial u}{\partial x}\frac{\partial^2 u}{\partial y^2}\right)= =\nu\frac{\partial^2 u}{\partial y^2}-\frac{\sigma B_0^2 u}{\rho_f}-\frac{\nu}{K}u-Fu^2 \tag{2}$$

$$u\frac{\partial T}{\partial x}+v\frac{\partial T}{\partial y}=\alpha\frac{\partial^2 T}{\partial y^2}+\tau\left[\frac{D_T}{T_\infty}\left(\frac{\partial T}{\partial y}\right)^2+D_B\frac{\partial C}{\partial y}\frac{\partial T}{\partial y}\right]+\frac{Q}{(\rho c)_f}(T-T_\infty) \tag{3}$$

$$u\frac{\partial C}{\partial x}+v\frac{\partial C}{\partial y}=\frac{D_T}{T_\infty}\frac{\partial^2 T}{\partial y^2}+D_B\frac{\partial^2 C}{\partial y^2} \tag{4}$$

$$\left.\begin{cases} u = u_w(x) = cx \\ v = v_w \\ -k\dfrac{\partial T}{\partial y} = h_f\left(T_f - T\right) \\ -D_B\dfrac{\partial C}{\partial y} = h_g\left(C_f - C\right)\end{cases}\right\} \text{at } y=0 \text{ where } T_f = T_0 + a_1 x \text{ and } C_f = C_0 + a_2 x \tag{5}$$

$$\left.\begin{cases} u \to 0 \\ T \to T_\infty = T_0 + d_1 x \\ C \to C_\infty = C_0 + d_2 x \end{cases}\right\} \text{ when } y \to \infty$$

Employing [25]:

$$\eta = y\sqrt{\frac{c}{\nu}},\ u = cxf'(\eta),\ v = -\sqrt{c\nu}\,f(\eta),\ \theta(\eta) = \frac{T - T_\infty}{T_f - T_0},\ \phi(\eta) = \frac{C - C_\infty}{C_f - C_0} \tag{6}$$

one obtains:

$$f''' + ff'' + \beta\left(2ff''' - f''^2 - ff^{iv}\right) - \left(\lambda + \mathrm{Ha}^2\right)f' - \left(1 + F_r\right)f'^2 = 0 \tag{7}$$

$$\theta'' + \mathrm{Pr}\left(f\theta' - f'\theta - S_1 f' + Nb\phi'\theta' + Nt\theta'^2 + \delta\theta\right) = 0 \tag{8}$$

$$\phi'' + \frac{Nt}{Nb}\theta'' + \mathrm{Sc}\left(f\phi' - f'\phi - S_2 f'\right) = 0 \tag{9}$$

$$f = S,\ f' = 1,\ \theta' = -\gamma_1[1 - S_1 - \theta(\eta)]$$

$$\phi' = -\gamma_2[1 - S_2 - \phi(\eta)] \text{ at } \eta = 0 \tag{10}$$

$$f' \to 0,\ \theta \to 0,\ \phi \to 0 \text{ as } \eta \to \infty \tag{11}$$

The variables entering in eqs. (7)-(10) are delineated:

$$\lambda = \frac{\nu}{Kc},\quad \beta = \frac{\alpha_1 c}{\mu},\quad S = \frac{-v_w}{\sqrt{c\nu}},\quad F_r = \frac{C_b x}{\sqrt{K}},\quad C_b = \frac{C_b^*}{x},\quad \mathrm{Ha}^2 = \frac{\sigma B_0^2}{\rho_f c}$$

$$Nt = \frac{\tau D_T\left(T_f - T_0\right)}{T_\infty \nu},\quad \mathrm{Pr} = \frac{\nu}{\alpha},\quad S_1 = \frac{d_1}{a_1},\quad Nb = \frac{\tau D_B\left(C_f - C_0\right)}{\nu} \tag{12}$$

$$S_2 = \frac{d_2}{a_2},\quad \mathrm{Sc} = \frac{\nu}{D_B},\quad \gamma_1 = \frac{h_f}{k}\sqrt{\frac{\nu}{c}},\quad \delta = \frac{Q}{c\left(\rho c\right)_f},\quad \gamma_2 = \frac{h_g}{D_B}\sqrt{\frac{\nu}{c}}$$

Local dimensional quantities (coefficient of drag-force, heat transfer rate, mass-transfer rate) are provided below:

$$C_{f_x} = \frac{\tau_w}{\rho u_w^2},\ \tau_w = \left[\mu\frac{\partial u}{\partial y} + \rho\alpha_1\left(2\frac{\partial u}{\partial x}\frac{\partial u}{\partial y} + u\frac{\partial^2 u}{\partial x \partial y}\right)\right]_{y=0} \tag{13a}$$

$$\mathrm{Nu} = \frac{xq_w}{k\left(T_f - T_\infty\right)},\ q_w = -k\left(\frac{\partial T}{\partial y}\right)_{y=0} \tag{13b}$$

$$\mathrm{Sh} = \frac{xq_m}{D_B\left(C_f - C_\infty\right)}, \quad q_w = -D_B\left(\frac{\partial C}{\partial y}\right)_{y=0} \tag{13c}$$

Coefficient of drag-force, $C_{fx}\mathrm{Re}_x^{0.5}$, heat-transfer rate, $\mathrm{NuRe}_x^{-0.5}$, and mass-transfer rate, $\mathrm{ShRe}_x^{-1/2}$, in non-dimensional forms are:

$$C_{f_x}\mathrm{Re}_x^{0.5} = [1+3\beta f'(0)]f''(0) \tag{14}$$

$$\frac{\mathrm{Nu}}{\mathrm{Re}_x^{0.5}} = -\frac{1}{1-S_1}\theta'(0) \tag{15}$$

$$\frac{\mathrm{Sh}}{\mathrm{Re}_x^{0.5}} = -\frac{1}{1-S_2}\phi'(0) \tag{16}$$

where $\mathrm{Re}_x = cx^2/\nu$.

Simulation procedure and outcomes

In the present article HAM is utilized to compute the non-linear problems, eqs. (7)-(11). This approach is based on semi-analytical technique which uses the concept of homotopy to produce convergent solutions. To fulfill the purpose, one can witness the ranges of $\hbar_\phi$, $\hbar_\theta$, and $\hbar_f$ obtained from the HAM code developed in Wolfram MATHEMATICA 12.0.1. The said ranges from fig. 2 are $-1.40 \le \hbar_\phi \le -0.55$, $-1.45 \le \hbar_\theta \le -0.35$, and $-1.0 \le \hbar_f \le -0.5$. Moreover, we also validate our convergent results by analyzing tab. 1. Convergence at 15th order approximation is developed, as shown in eqs. (7)-(9). An excellent agreement is achieved with [19], tab. 2. Effects of various parameters like Pr, Ha, S_1, S_2, δ, γ_1, γ_2, Nt, Nb, and Sc on $\theta(\eta)$, $\phi(\eta)$, $C_{fx}\mathrm{Re}_x^{0.5}$, $\mathrm{NuRe}_x^{-0.5}$, and $\mathrm{ShRe}_x^{-0.5}$ are expounded in figs. 3-16.

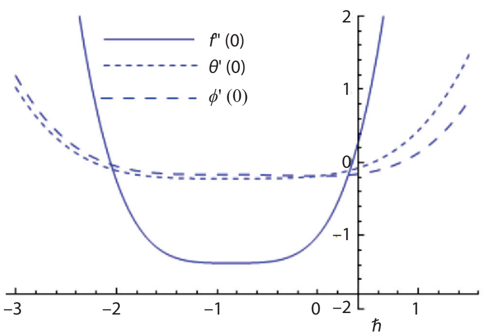

Figure 2. The $\hbar$-curve plot of f, θ, and ϕ

Figure 3 is plotted to capture the effects of Nt on $\theta(\eta)$. This graph show that the enhancement of Nt results in the higher temperature. The variations of $\theta(\eta)$ against various values of Nb are displayed in fig. 4. The $\theta(\eta)$ rises as expected. This implies that the transportation of

Table 1. Convergent outcomes for distinctive order approximations considering Nt = Ha = Nb = F_r = 0.1, $S_2 = \beta_1 = \delta = S_1 = 0.2$, $\gamma_2 = \gamma_1 = 0.3$, $S = 0.4$, $\lambda = 0.5$, Sc = 0.8, and Pr = 1.2

Order of approximations	$-f''(0)$	$-\theta'(0)$	$-\phi'(0)$
1	1.2503	0.2065	0.1844
4	1.3731	0.2190	0.1649
9	1.3745	0.2194	0.1637
15	1.3745	0.2194	0.1637
25	1.3745	0.2194	0.1637
35	1.3745	0.2194	0.1637
40	1.3745	0.2194	0.1637

Table 2. Comparative values for $-f''(0)$ considering λ estimations when $F_r = \text{Ha} = S = \beta = 0.0$

	$-f''(0)$	$-f''(0)$
λ	[11]	Present
0.0	1.0000	1.0000
0.50	1.0198	1.0198
1.00	1.1180	1.1180

the nanoparticle upsurges for larger values of Nb. Such augmentation in heat transportation is owing to manifestation of Brownian diffusion, which causes exhilaration in nanoparticles. The deviation of $\theta(\eta)$ against S_1, γ_1, Pr, and δ is depicted in figs. 5-8. It can be noted that there is a temperature drop against increasing estimations of S_1 and Pr, whereas an opposite situation is witnessed for higher γ_1 and δ. Figure 9 is presented to capture the influence of Nt on $\phi(\eta)$. One can explicate that $\phi(\eta)$ is an increasing function of Nt. This rise is due to the generation of thermophoretic force for large Nt. This force aids nanoparticles movement in the less heated surroundings. The fluctuations of $\phi(\eta)$ for different Schmidt number are described in fig. 10. Diminution of $\phi(\eta)$ is countersigned for higher values of Schmidt number. This result is due to the reduction in mass diffusivity for greater Schmidt number. Figures 11-13 elucidates the trend of $\phi(\eta)$ *vs.* S_2, γ_2, and Nb. The S_2 and Nb resist $\phi(\eta)$ while γ_2 assist it. Figure 14 is plotted to illustrate the impact of Ha and λ on $C_{fx}\text{Re}_x^{0.5}$. It is highlighted that Ha and λ are assistive factors for the physical quantity $C_{fx}\text{Re}_x^{0.5}$. Characteristics of Nb, Nt, γ_2, and Sc on $\text{NuRe}_x^{-0.5}$ and $\text{ShRe}_x^{-0.5}$ are delineated via figs. 15 and 16. As anticipated $\text{NuRe}_x^{-0.5}$ lessens for higher Nt and Nb while opposite trend is found when γ_2 and Sc are augmented.

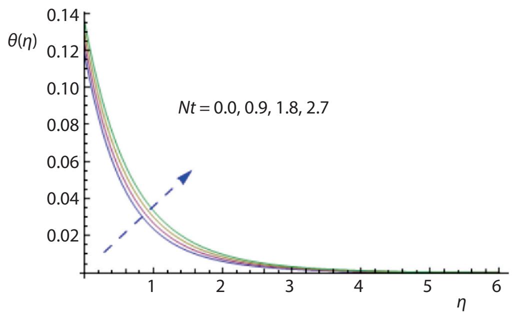

Figure 3. The θ via Nt

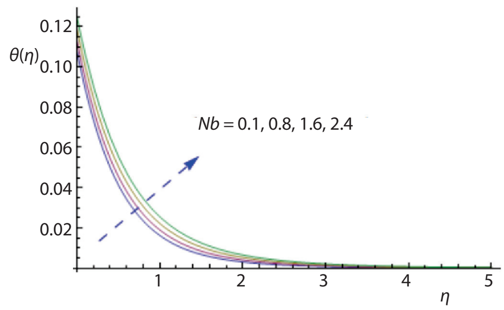

Figure 4. The θ via Nb

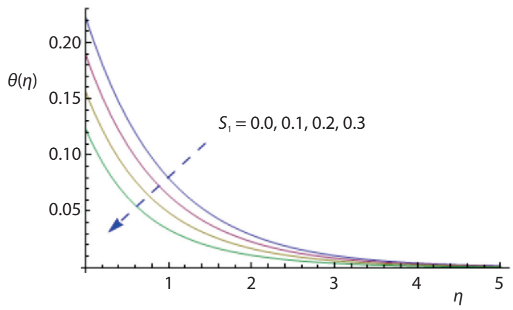

Figure 5. The θ via S_1

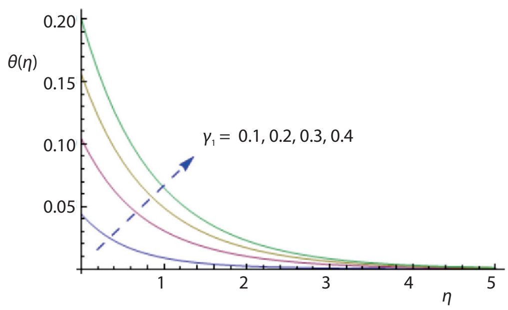

Figure 6. The θ via γ_1

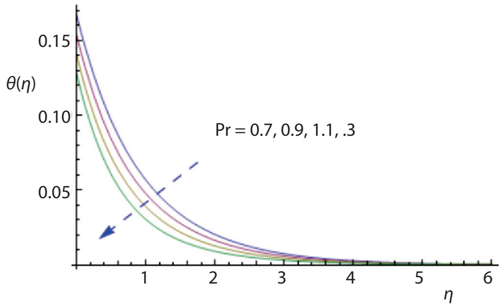

Figure 7. The θ via Pr

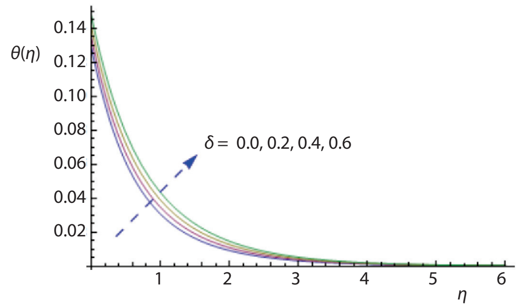

Figure 8. The θ via δ

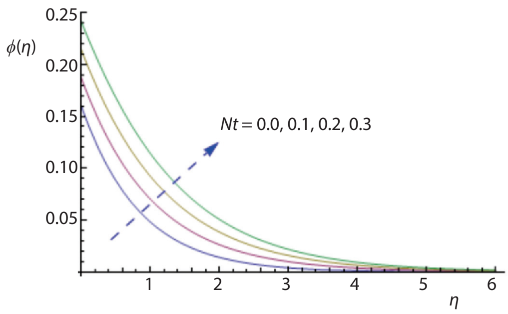

Figure 9. The ϕ via Nt

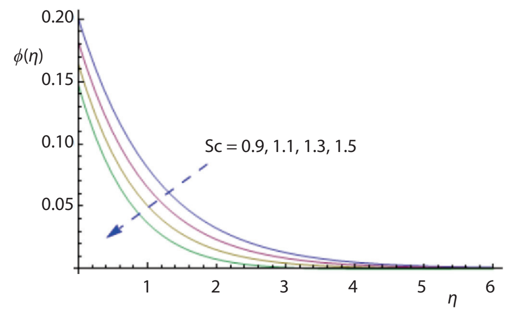

Figure 10. The ϕ via Sc

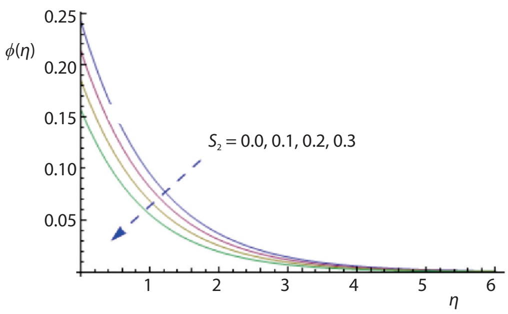

Figure 11. The ϕ via S_2

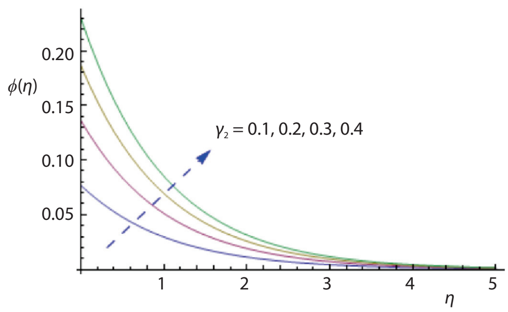

Figure 12. The ϕ via γ_2

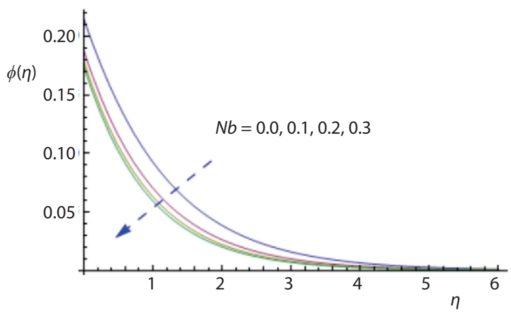

Figure 13. The ϕ via Nb

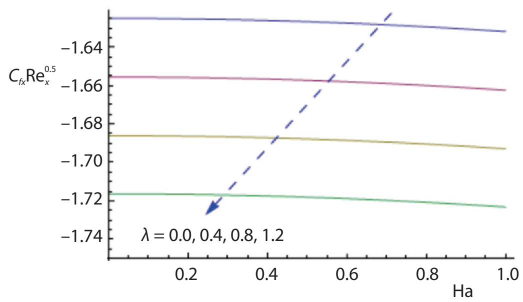

Figure 14. The $C_{fx}\mathrm{Re}_x^{0.5}$ via λ and Ha

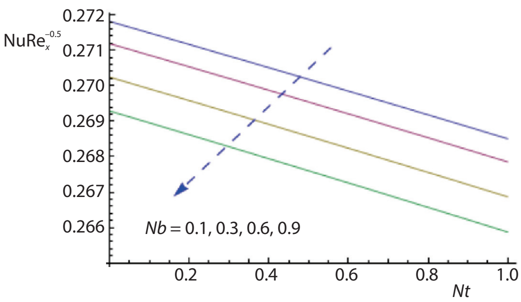

Figure 15. The NuRe$_x^{-0.5}$ via Nt and Nb

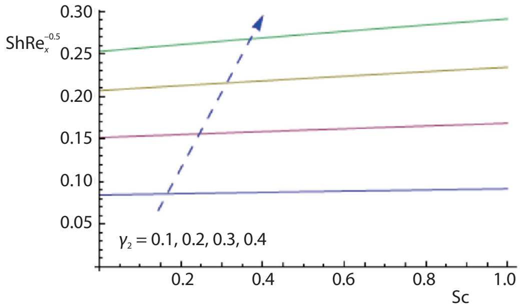

Figure 16. The ShRe$_x^{-0.5}$ via γ_2 and Sc

Conclusions

In the present work the MHD of a viscoelastic nanoliquid with non-Darcian properties is explored. The integration of convective conditions and stratifications with such fluid-flow problem make it even more novel. The resulting non-linear ODE is solved by famous HAM technique. The Nt and Nb are established as couple of assistive factors for $\theta(\eta)$ as compared to NuRe$_x^{-0.5}$. The ShRe$_x^{-0.5}$ is an increasing function of Sc and γ_2. Concentration and temperature diminishes due to stratifications and convective conditions. It is worth-mentioning that modeled analysis corresponds to viscous nanoliquid situation when material parameter $\beta = 0$.

Acknowledgment

The authors wish to express their thanks for the financial support received from King Fahd University of Petroleum and Minerals under grant IN171009.

Nomenclature

a_1, d_1, a_2, d_2 – non-dimensional constants
B_0 – magnetic field intensity
C – nanoparticle concentration
C_b – drag coefficient
C_b^* – coefficient of drag per length
C_f – hot liquid concentration
C_∞ – ambient liquid concentration
C_0 – reference concentration
$C_{fx}\mathrm{Re}_x^{0.5}$ – non-dimensional drag force
c – stretching rate
D_B – Brownian movement coefficient
D_T – thermophoresis diffusion coefficient
F_r – local inertia coefficient
$f'(\eta)$ – non-dimensional velocity
Ha – Hartman number
K – porous medium permeability
k – hermal conductivity
Nb – Brownian diffusion factor
Nt – thermophoretic variable
NuRe$_x^{-0.5}$ – non-dimensional heat transfer rate
Pr – Prandtl number
Q – uniform heat sink/source
Re$_x$ – Reynolds numbers
S – mass-transfer parameter
Sc – Schmidt number
ShRe$_x^{-0.5}$ – non-dimensional mass-transfer rate
S_1 – thermal stratified variable
S_2 – solutal stratified variable
T – temperature
T_f – hot liquid temperature
T_0 – reference temperature
T_∞ – ambient liquid temperature
u_w – stretchable velocity
u, v – components of velocity
v_w – mass-transfer velocity
x, y – space co-ordinates
$\hbar_f, \hbar_\theta, \hbar_\phi$ – auxiliary parameters

Greek symbols

α – thermal diffusivity
α_1 – normal stress moduli
β – second-grade liquid parameter
γ_1 – thermal Biot number
γ_2 – concentration Biot number
δ – heat sink/source factor
η – non-dimensional variable
$\theta(\eta)$ – dimensionless temperature
λ – porosity factor
μ – dynamic viscosity
ν – kinematic viscosity

ρ_f – base liquid density
$(\rho c)_f$ – liquid heat capacity
σ – electrical conductivity
τ – ratio of heat capacity
$\phi(\eta)$ – dimensionless concentration

References

[1] Choi, S. U. S., Eastman, J. A., Enhancing Thermal Conductivity of Fluids with Nanoparticles: *Proceedings,* 1995 ASME International Mechanical Engineering Congress and Exposition, San Francisco, Cal., USA, *ASME, FED 231/MD*, *66*, 1995, pp. 99-105
[2] Yu, W., *et al*., Review and Comparison of Nanofluid Thermal Conductivity and Heat Transfer Enhancements, *Heat Transfer Eng*., *29* (2008), 5, pp. 432-460
[3] Buongiorno, J., Hu, L. W., Nanofluid Heat Transfer Enhancement for Nuclear Reactor Applications, *Proceedings,* 2nd Micro/Nanoscale Heat and Mass Transfer International Conference, Shangai, China, ASME, 2009, pp. 517-522
[4] Sulochana, C., Sandeep, N., Stagnation Point Flow and Heat Transfer Behavior of Cu-water Nanofluid Towards Horizontal and Exponentially Stretching/Shrinking Cylinders, *Appl. Nanosci*., *6* (2016), 3, pp. 451-459
[5] Waqas, M., *et al*., Numerical Simulation for Magneto Carreau Nanofluid Model with Thermal Radiation: A Revised Model, *Computer Methods Appl. Mech. Eng*., *324* (2017), Sept., pp. 640-653
[6] Shen, B., *et al*., Bioconvection Heat Transfer of a Nanofluid over a Stretching Sheet with Velocity Slip and Temperature Jump, *Thermal Science*, *21* (2017), 6A, pp. 2347-2356
[7] Waqas, M., *et al*., Simulation of Magnetohydrodynamics and Radiative Heat Transport in Convectively Heated Stratified Flow of Jeffrey Nanofluid, *Journal of Physics and Chemistry of Solids*, *133* (2019), Oct., pp. 45-51
[8] Waqas, M., *et al*., Modelling and Analysis for Magnetic Dipole Impact in Non-Linear Thermally Radiating Carreau Nanofluid-Flow Subject to Heat Generation, *Journal of Magnetism and Magnetic Materials*, *485* (2019), Sept., pp. 197-204
[9] Dogonchi, A. S., *et al*., Shape Effects of Copper-Oxide (CuO) Nanoparticles to Determine the Heat Transfer Filled in a Partially Heated Rhombus Enclosure: CVFEM Approach, *International Communications in Heat and Mass Transfer*, *107* (2019), Oct., pp. 14-23
[10] Waqas, M., *et al*., Transportation of Radiative Energy in Viscoelastic Nanofluid Considering Buoyancy Forces and Convective Conditions, *Chaos, Solitons and Fractals*, *130* (2020), Jan., 109415
[11] Umavathi, J. C., Hemavathi, K., Flow and Heat Transfer of Composite Porous Medium Saturated with Nanofluid, *Propulsion and Power Research*, *8* (2019), 2, pp. 173-181
[12] Darcy, H., *Les Fontaines Publiques De La Ville De Dijon*, Victor Dalmont, Paris, 1856
[13] P. Forchheimer, Wasserbewegung durch boden (in German), *Zeitschrift des Vereins deutscher Ingenieure, 45* (1901), pp. 1782-1788
[14] Muskat, M., Meres, W., The Flow of Heterogeneous Fluids through Porous Media, *Journal Appl. Phys., 7* (1936), 346
[15] Sadiq, M. A., *et al*., Importance of Darcy-Forchheimer Relation in Chemically Reactive Radiating Flow Towards Convectively Heated Surface, *Journal Mol. Liq*., *248* (2017), Dec., pp. 1071-1077
[16] Hayat, T., Peristalsis of Eyring-Powell Magneto Nanomaterial Considering Darcy-Forchheimer Relation, *International Journal of Heat and Mass Transfer*, *115* (2017), Part A, pp. 694-702
[17] Hayat, T., *et al*., Effectiveness of Darcy-Forchheimer and Non-Linear Mixed Convection Aspects in Stratified Maxwell Nanomaterial Flow Induced by Convectively Heated Surface, (ed. English), *Applied Mathematics and Mechanics*, *39* (2018), Aug., pp. 1373-1384
[18] Sadiq, M. A., *et al*., Modelling and Analysis of Maxwell Nanofluid Considering Mixed Convection and Darcy-Forchheimer Relation, *Applied Nanoscience*, *9* (2019), Feb., pp. 115-1162
[19] Waqas, M., *et al*., Darcy-Forchheimer Stratified Flow of Viscoelastic Nanofluid Subjected to Convective Conditions, *Applied Nanoscience*, *9* (2019), Sept., pp. 2031-2037
[20] Khan, M. I., *et al*., The Role of γAl_3O_3-H_2O and γAl_2O_3-$C_2H_6O_2$ Nanomaterials in Darcy-Forchheimer Stagnation Point Flow: an Analysis Using entropy Optimization, *Int. J. Thermal Sci*., *140* (2019), June, pp. 20-27
[21] Liao, S. J., An Optimal Homotopy-Analysis Approach for Strongly Non-Linear Differential Equations, *Commun. Non-linear Sci. Numer. Simulat.*, *15* (2010), 8, pp. 2003-2016
[22] Waqas, M., *et al*., Magnetohydrodynamic (MHD) Mixed Convection Flow of Micropolar Liquid Due to Non-Linear Stretched Sheet with Convective Condition, *Int. J. Heat and Mass Transfer*, *102* (2016), Nov., pp. 766-772

[23] Qayyum, S., *et al.*, Non-Linear Thermal Radiation and Magnetic Field Effects on the Flow Carreau Nanofluid with Convective Conditions, *Thermal Science*, *24* (2018), 2B, pp. 1217-1228
[24] Waqas, M., *et al*., A Generalized Fourier and Fick's Perspective for Stretching Flow of Burgers Fluid with Temperature-Dependent Thermal Conductivity, *Thermal Science*, *23* (2018), 6A, pp. 3425-3432
[25] Anwar, M. I., *et al*., A Modified Fourier-Fick Analysis for Modelling Non-Newtonian Mixed Convective Flow Considering Heat Generation, *Thermal Science*, *24* (2019), 2B, pp. 1381-1387

Paper submitted: July 8, 2019
Paper revised: September 18, 2019
Paper accepted: September 25, 2019